

# Radiotherapy beyond cancer: Target localization in real-time MRI and treatment planning for cardiac radiosurgery

Ipsen S<sup>1,2</sup>, Blanck O<sup>3</sup>, Oborn B<sup>4</sup>, Bode F<sup>5</sup>, Liney G<sup>6</sup>, Hunold P<sup>7</sup>, Rades D<sup>8</sup>, Schweikard A<sup>2</sup>, Keall P J<sup>1</sup>

1 Radiation Physics Laboratory, Sydney Medical School, The University of Sydney, NSW 2006, Australia

2 Institute for Robotics and Cognitive Systems, University of Luebeck, Luebeck, Germany

3 Department of Radiation Oncology, University of Luebeck and University Medical Center Schleswig-Holstein, Campus Luebeck, Germany

4 Illawarra Cancer Care Centre (ICCC), Wollongong, NSW 2500, Australia and Centre for Medical Radiation Physics (CMRP), University of Wollongong, Wollongong, NSW 2500, Australia

5 Medical Department II, University of Luebeck and University Medical Center Schleswig-Holstein, Campus Luebeck, Germany

6 Ingham Institute for Applied Medical Research, Liverpool Hospital, Liverpool, NSW 2170, Australia

7 Department of Radiology and Nuclear Medicine, University of Luebeck and University Medical Center Schleswig-Holstein, Campus Luebeck, Germany

8 Department of Radiation Oncology, University of Luebeck and University Medical Center Schleswig-Holstein, Campus Luebeck, Germany

**Purpose:** Atrial fibrillation (AFib) is the most common cardiac arrhythmia that affects millions of patients world-wide. AFib is usually treated with minimally-invasive, time consuming catheter ablation techniques. While recently non-invasive radiosurgery to the pulmonary vein antrum (PVA) in the left atrium (LA) has been proposed for AFib treatment, precise target location during treatment is challenging due to complex respiratory and cardiac motion. An MRI-Linac could solve the problems of motion tracking and compensation using real-time image guidance. In this study, we quantified target motion ranges on cardiac MRI and analyzed the dosimetric benefits of margin reduction assuming real-time motion compensation was applied.

**Method:** For the imaging study, six human subjects underwent real-time cardiac MRI under free breathing. The target motion was analyzed retrospectively using a template matching algorithm. The planning study was conducted on a CT of an AFib patient with a centrally located esophagus undergoing catheter ablation, representing an ideal case for cardiac radiosurgery. The target definition was similar to the ablation lesions at the PVA created during catheter treatment. Safety margins of 0 mm (perfect tracking) to 8 mm (untracked respiratory motion) were added to the target, defining the PTV. For each margin a 30 Gy single fraction IMRT plan was generated. Additionally, the influence of 1 T and 3 T magnetic fields on the treatment beam delivery was simulated using Monte Carlo calculations to determine the dosimetric impact of MRI guidance for two different linac positions.

**Results:** Real-time cardiac MRI showed mean respiratory target motion of 10.2 mm (superior-inferior), 2.4 mm (anterior-posterior) and 2 mm (left-right). The planning study showed that increasing safety margins to encompass untracked respiratory motion leads to overlapping structures even in the ideal scenario, compromising either normal tissue dose constraints or PTV coverage. The magnetic field caused a slight increase in the PTV dose with the in-line MRI-Linac configuration.

**Conclusions:** Our results indicate that real-time tracking and motion compensation is mandatory for cardiac radiosurgery and MRI-guidance is feasible, opening the possibility of treating cardiac arrhythmia patients completely non-invasively.

Key words: Atrial fibrillation, cardiac radiosurgery, real-time tracking, image guidance, MRI-Linac

## 1. INTRODUCTION

45 Atrial fibrillation (AFib) is the most common type of cardiac arrhythmia and is considered a growing epidemic, with estimates suggesting that up to 7M Americans<sup>1</sup> and more than 6M Europeans<sup>2</sup> are affected. Prevalence numbers are expected to at least double over the next 50 years. AFib has been shown to increase the risk of ischemic strokes and heart failure by up to five times and is the underlying cause for 20% of all strokes.<sup>1</sup> AFib is caused by aberrant electrical impulses originating from the atria of the heart, mostly from the pulmonary veins entering the left atrium (LA). These signals disturb the natural sinus rhythm of the heart, leading to inefficient atrial contractions at high frequencies (more  
50 than 600 beats per minute) which favor blood clot formation and irregular heartbeats.

A well-established yet highly complex and time-consuming approach for the treatment of AFib patients is the electrical isolation of the pulmonary veins through catheter ablation. Currently, major complications occur in about 6% of CA procedures, some of them life-threatening conditions such as cardiac tamponade, a rupture of the heart muscle leading to major bleedings, or esophageal injury. Especially geriatric patients and those with cardiac comorbidities have low success rates and are mostly ineligible for this invasive and highly stressful procedure.<sup>3</sup>  
55

Radiosurgery is currently being used in clinical practice to treat solid tumors throughout the body with high dose ionizing radiation. For an AFib treatment, radiosurgery could hold the ability to create lesions similar to catheter ablation but non-invasively. Its potential has been investigated in several animal studies using a robotic radiosurgery platform<sup>4-6</sup> (CyberKnife, Accuray Inc., Sunnyvale, USA) and an image-guided radiotherapy system<sup>7</sup> (Varian Inc., Palo Alto, USA). The creation of fibrotic lesions in the heart was demonstrated in both systems. The CyberKnife was also used in the first reported human treatments for ventricular tachycardia<sup>8,9</sup> with positive early outcomes Reported.  
60

Although the results of the previous radiation treatments of AFib have been promising, there are a number of limitations of the technologies used. The CyberKnife uses respiratory tracking software based on a correlation model between a continuous external breathing signal, i.e. the chest motion observed with an infrared camera, and internal position data acquired with discrete 2D x-ray image pairs over the course of treatment.<sup>10</sup> The inevitable surgical implantation of radiopaque markers into the heart for x-ray-based tracking undermines the non-invasiveness of the AF treatment and is a mere surrogate for the actual target position. Differential motion of the markers and the target cannot be accounted for and is uncompensated.<sup>11</sup> The most recent study<sup>7</sup> performed a completely non-invasive procedure to investigate the optimal therapeutic dose necessary to create atrial lesions, however without using any real-time guidance. The main limitation of the previously published approaches is the lack of accurate real-time motion data for the continuous tracking of targets moving with cardiac contraction and respiration.  
65  
70

A potential imaging modality that provides high resolution images with good and variable soft tissue contrast without requiring additional imaging dose is magnetic resonance imaging (MRI). To date, no real-time localization method for cardiac targets in combination with motion compensation for radiotherapy exists. We therefore investigate a novel approach to a non-invasive real-time image-guided AFib treatment using an integrated MRI linear accelerator (MRI-Linac). Recent research towards MRI guidance during radiotherapy demonstrated that tracking of three-dimensional organ motion in abdominal regions, e.g. the kidneys, can be implemented using multiple orthogonal interleaved 2D planes and fast template matching.<sup>12</sup> We hypothesize that this non-ionizing, non-invasive imaging technique could also be used for real-time tracking of the heart to treat AFib. *Figure 1* shows a comparison between a catheter ablation procedure and the potential treatment scenario with an MRI-Linac. Catheter ablation is an extensive and expensive procedure – it can take several hours and cost up to \$50,000 USD.<sup>13</sup> We estimate that MRI-guided cardiac radiosurgery could be performed in less than one hour while being completely non-invasive and potentially of similar cost-effectiveness as lung SBRT compared to radiofrequency ablation.<sup>14</sup>  
75  
80

In this letter, we report on our initial findings, the challenges and potential future directions of cardiac radiosurgery.

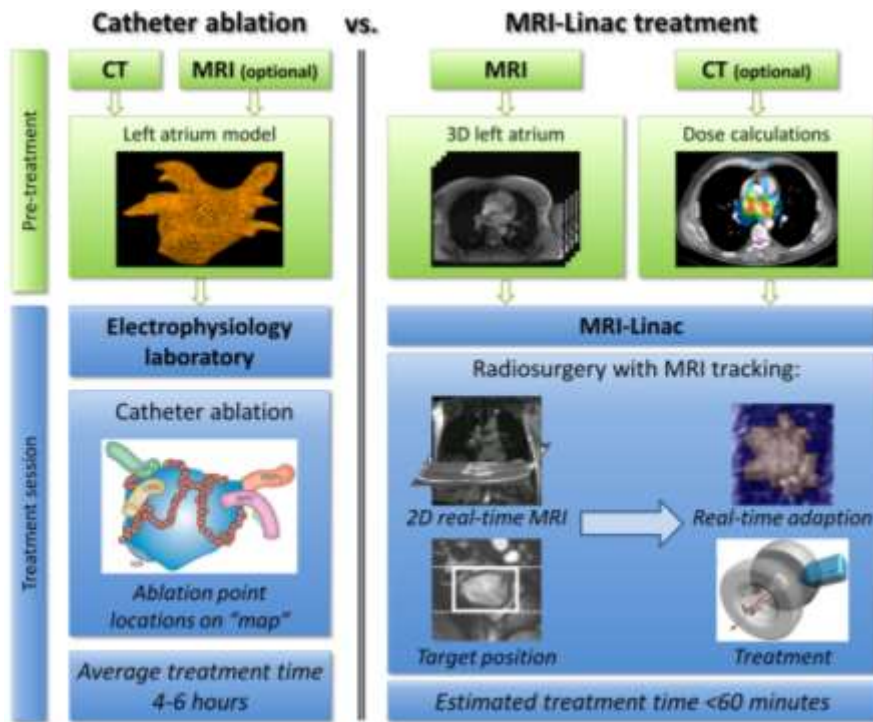


Figure 1: Comparison between a conventional catheter ablation procedure and the investigated treatment approach using an integrated MRI-Linac with real-time guidance. The proposed method could reduce treatment time substantially.

## 2. METHODS

### a. Real-time cardiac MRI

The intended use of MRI for real-time tracking demands a high spatiotemporal resolution. In contrast to conventional cardiac sequences, images are acquired during free breathing to simulate a realistic treatment scenario in an MRI-Linac. All the MRI scans were acquired on a 3T Magnetom Skyra (Siemens Healthcare, Erlangen, Germany) using a fast gradient echo sequence based on modified balanced steady state free precession (TrueFISP - Fast Imaging with Steady state Precession) with the following parameters (note variations between scans): TE/TR = 1.3-1.5/50-115 ms, flip angle = 43°, slice thickness = 6-8 mm, in-plane voxel size = 1.4-2 mm, field-of-view (FOV) = 260-380 × 340-380 mm<sup>2</sup>, parallel imaging factor 2. An 18-channel long body-coil was used for signal detection. ECG gating / triggering was not required for the real-time free breathing scans.

Six male healthy volunteers underwent real-time cardiac MRI scans to initially assess the range of observable target motion. The motion extent is directly related to the margin size that needs to be added to the target structure for treatment planning. All volunteers were imaged in coronal, sagittal and/or transverse planes (see Figure 2) to cover the three-dimensional motion path of the LA in all breathing phases. The cine MRI scans consisted of 50-256 frames during normal free breathing to quantify motion in superior-inferior (S-I), anterior-posterior (A-P) and left-right (L-R) direction over several breathing cycles.

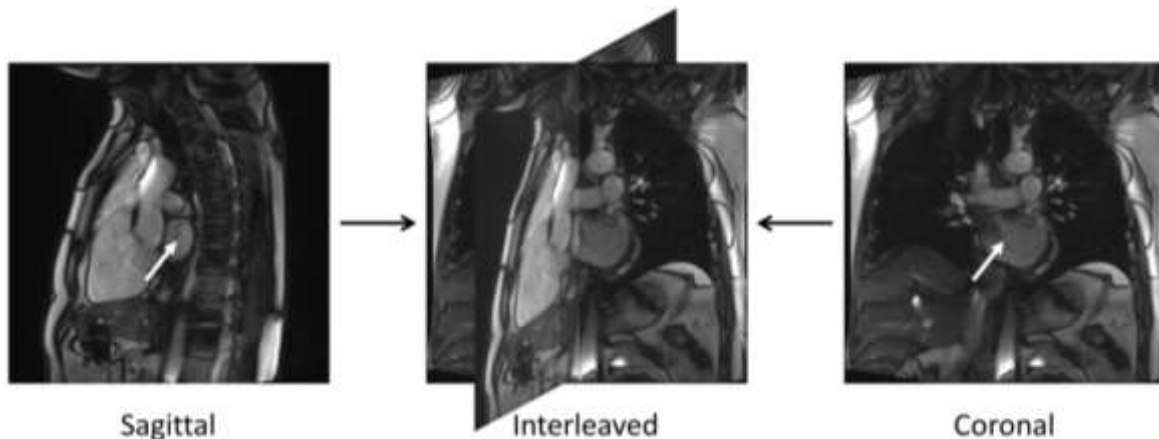


Figure 2: Single frames of a cine MRI TrueFISP acquisition. The left atrium is clearly visible in both plane orientations, sagittal and coronal, as indicated by the white arrows. The center image shows how the orthogonal imaging planes interleave.

Respiratory motion, representing the main driver of target displacement, was assessed using retrospective analysis with rigid TM. Cardiac contractile motion was not considered in these initial experiments. The left atrium (LA), representing the treatment region, was delineated manually in the first image  $I_1$  to create the template  $T$ . The sum of squared differences was calculated as a similarity metric between the subsequent target frames  $I_i$  and  $T$ , the lowest value indicating the best match. The average template shift  $\mu$  in superior-inferior (S-I), anterior-posterior (A-P) and left-right (L-R) direction corresponds to the difference of the mean positions at the extrema of the breathing cycle, i.e. end-inhalation versus end-exhalation, over the number of observed cycles during a single cine sequence. By multiplying the average shift of the template (see Figure 3) with the pixel spacing of the MRI scan, the target motion in millimeters can be approximated.

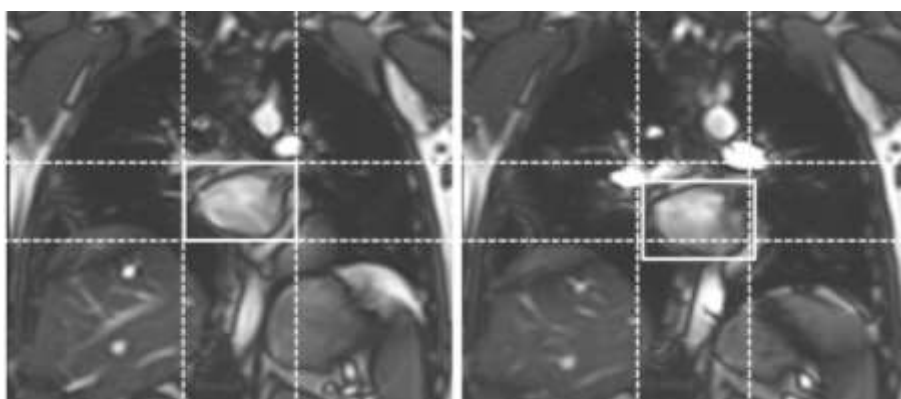


Figure 3: The template shift during one breathing cycle in the coronal plane. The mean template shift  $\mu$  is calculated over all observed breathing cycles by multiplying the pixel shift with the pixel spacing.

### b. Treatment plan generation

Treatment plans were created for one patient with a centrally located esophagus undergoing catheter ablation for AF using the Pinnacle treatment planning system (Philips Radiation Oncology Systems, Fitchburg, WI). A cardiac-gated CT scan was acquired on a Somatom Definition AS (Siemens Healthcare, Erlangen, Germany) with a resolution of  $0.8 \times 0.8 \times 1 \text{ mm}^3$  (skin to skin reconstruction), ten respiratory phases and intravenous contrast agent for visualizing the left atrial target. Contouring and planning were performed on the mid-inhalation breathing phase.

The target structure was defined as a circumferential lesion in the left and right pulmonary vein antrum, respectively, with the goal of blocking the electrical conduction from the pulmonary veins to the LA. The resulting clinical target volumes (CTVs) were similar to lesion sets created with catheter ablation (see Figure 4) which can be precisely contoured in the contrast enhanced CT scan. The organs at risk (OARs) included the esophagus, the airways (containing trachea and main left and right bronchus), the aorta, the spinal cord, the heart, the lung and the skin. To compensate for the artificially enhanced contrast of the blood pool in the planning CT, the attenuation values of the heart and the aorta were set to the mean value of the myocardium.

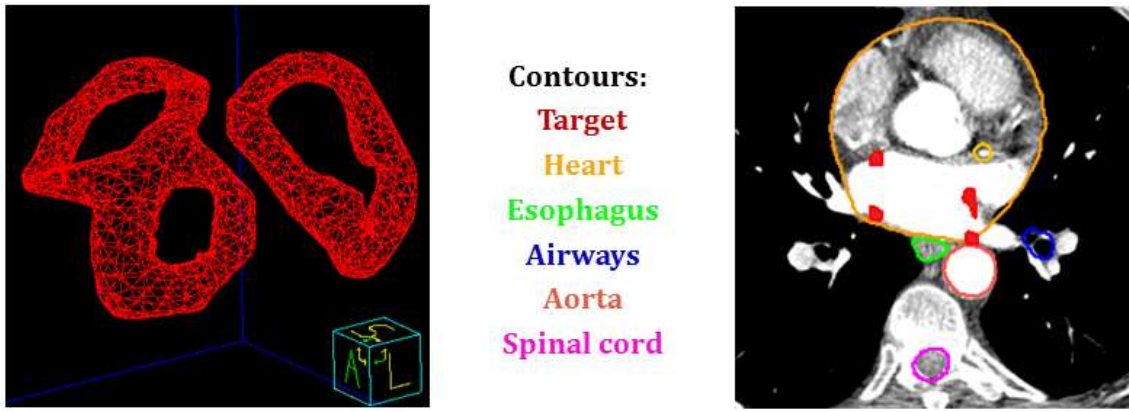


Figure 4: The target structure for radiosurgical AFib treatment is located at the antral region of the pulmonary veins (intersection with the left atrium). A three dimensional mesh representation of the target structure is shown on the left. The right shows the treatment region on a contrast-enhanced, cardiac gated CT scan with contours of the target and the major OARs (heart, esophagus, airways, aorta and spinal cord). The target structures (left) are shown as four discrete regions in this 2D axial view.

We enlarged the CTV to generate the planning target volume (PTV) based on various margins to encompass untracked respiratory motion. In this first planning study, five plans with different margin sizes (0, 1, 3, 5, 8 mm) were created. The stepwise increase of the margin size ranged from 0mm, representing perfect tracking, up to 8 mm based on the MRI respiratory target motion assessed in this work (see results section) and published literature.<sup>15</sup> The assumption is that if treatment planning is performed on mid-inhalation phase and the absolute magnitude of respiratory motion is about 10-15 mm, then 8 mm isotropic margins would encompass the observed motion. Eleven intensity modulated (IMRT) fields with a 120-leaf MLC were used to generate treatment plans with 6 MV photons. Based on previous animal studies without tracking and 4D dose simulation, each plan prescribed 30 Gy to 95% of the PTV in a single fraction, treating both vein locations simultaneously.<sup>7,26</sup> The maximum dose threshold was set to 37.5 Gy. Dose tolerance limitations for the OARs<sup>16</sup> were based on current radiosurgery practice for single fraction lung stereotactic body radiotherapy (SBRT) and RTOG 0915.

When investigating this new potential indication for MRI-guided radiosurgery, it is crucial to calculate and quantify the dosimetric impact of the magnetic fields on beam delivery. Therefore, we performed Monte Carlo calculations based on the software toolkit Geant4<sup>17</sup> for particle transport simulations. Two different orientations of the magnetic field are under development; parallel and perpendicular to the therapy beam direction. Both were studied here. Magnetic field strengths of 1 T, corresponding to a model MRI-Linac, and 3 T, the scanner field strength used for the cardiac MRI studies, were simulated.

### 3. RESULTS

#### a. Left atrial motion assessment using real-time MRI

The motion of the LA was measured using template matching on cine MRI scans of the beating heart during free breathing. The focus of this initial study was to quantify the impact of respiratory motion on the target region. By reducing the matching complexity to rigid transformations, we avoided most of the influence of cardiac contractile motion. Note that the motion was measured retrospectively on one imaging plane at a time and limited to the LA. Differential motion of the distal pulmonary veins and the complex contraction pattern of the LA were not investigated in this study.

The results of the motion assessment are shown in Table 1. As expected, the direction of highest motion extent is in the S-I plane which can be measured in both the coronal and sagittal MRI planes. The left atrial motion in A-P and L-R direction was four times smaller than S-I motion. The variance reflects the variability between different breathing cycles. The respiratory motion magnitude and also the cycle length varied highly among individuals and even within a single acquisition. It is possible that patients with cardiac or pulmonary comorbidities show shallower breathing with shorter respiratory periods.

Table 1: Overview of measured three-dimensional LA motion for the different MRI scan plane orientations.

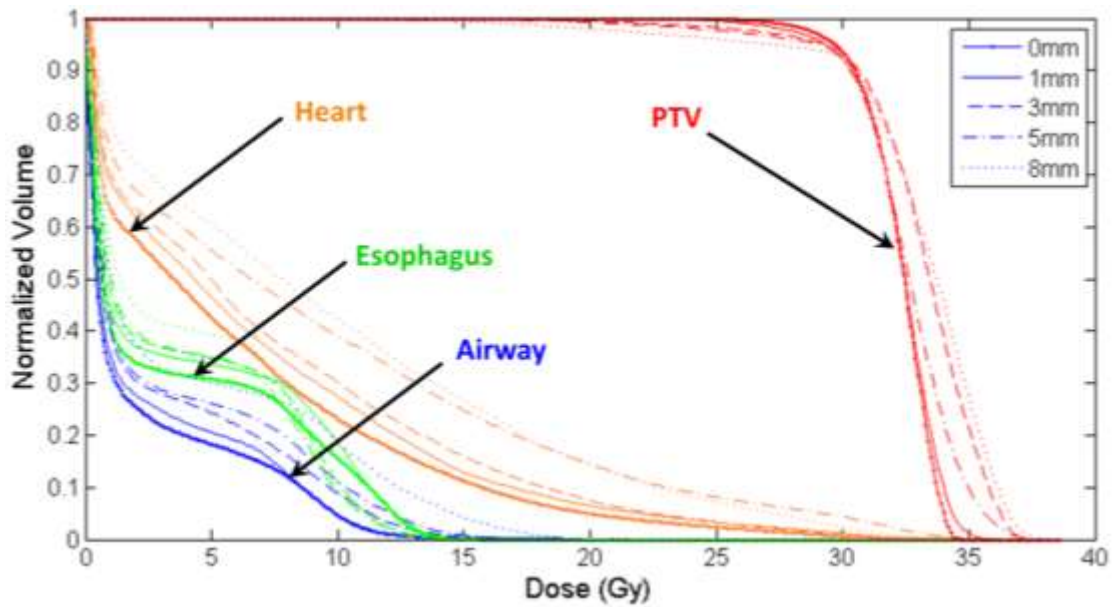
Scan plane	Number of	Number of	Measured	Template shift $\mu$
------------	-----------	-----------	----------	----------------------

orientation	subjects	scans	direction	±standard deviation (mm)
Axial	5	6	A-P	2.3 ± 1.0
			L-R	1.1 ± 0.9
Coronal	2	6	S-I	9.9 ± 5.2
			L-R	3.0 ± 2.0
Sagittal	4	4	S-I	11.6 ± 3.1
			A-P	2.7 ± 0.5
<b>Overall</b>	8	10	<b>S-I</b>	<b>10.2 ± 3.0</b>
		10	<b>A-P</b>	<b>2.4 ± 1.4</b>
		12	<b>L-R</b>	<b>2.0 ± 1.2</b>

## b. Cardiac radiosurgery treatment planning

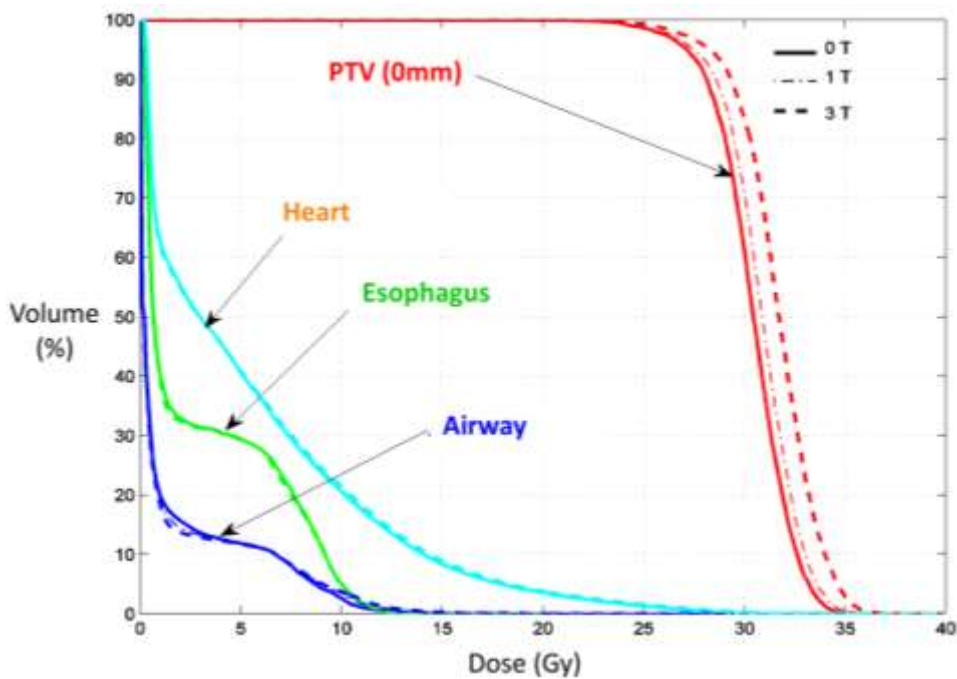
The results of the treatment planning study for AFib targets with variable margins in the left atrium of the heart are illustrated in *Figure 5*. The dose-volume histogram (DVH) includes the target and the main critical structures (heart, esophagus and airway). These structures were chosen for their high radiosensitivity and their close proximity to the target which makes exceeding the pre-defined dose limitations more likely. In this initial planning experiment, it was possible to achieve an esophagus maximum dose  $\leq 15.5$  Gy and an airway dose well below 22 Gy for all margin sizes. The maximum point doses and also the dose-volume values to the OARs other than the heart and esophagus were found to be within acceptable limits except for the airway dose in the 8 mm margin plan which exceeded the recommended tolerance dose of 10.5 Gy to a 4 cm<sup>3</sup> volume by over 30%. We also observed a 10% drop in the D<sub>95%</sub> to the target, decreasing from 30 Gy for 0 mm margins to 27 Gy for 8 mm. The maximum point dose to the target exceeded the pre-defined threshold of 37.5 Gy in the 5 and 8 mm plans. The heart dose was relatively high, even for the 0 mm plan, and increased further with broader margins. These values give an indicator for the benefits of margin size minimization in order to spare healthy tissue, ensure sufficient target coverage and avoid extreme hot spots. Our solution to reduce margins is real-time tracking with MRI-guidance.

*Figure 6* shows the DVH for a simulated AFib treatment plan with no margins added to the target structure in an in-line configuration of an MRI-Linac. 0 T corresponds to a conventional, non-MRI treatment. When performing real-time tracking with MRI-guidance, we introduce magnetic fields into the beam delivery and dose deposition process. The impact of a 1 T and 3 T field is most dominant in the in-line set-up. We observed a mild increase in the mean PTV dose of 0.4 Gy (1.3%) at 1 T and 1.3 Gy (4.3%) at 3 T which is caused by a reduction of lateral scatter due to the focusing effect of the magnetic field on secondary electrons. Changes to the critical structures and the effects of a perpendicular configuration were minimal, with the Lorentz force effects observed for individual beams. However, these effects are partially cancelled by opposing beams. These simulations indicate that MRI-guidance does not drastically interfere with treatment delivery for cardiac radiosurgery. It even increases target dose in the in-line configuration so that further optimization might lead to a reduction in OAR dose.



195

Figure 5: Dose-volume histogram (DVH) for AFib treatment plans with varying margins. The target-PTV margin size ranged from 0 mm (perfect tracking), indicated by solid lines, to 8 mm (uncompensated respiratory motion), dotted lines. The target (PTV - red) and the main critical structures (heart - orange, esophagus - green, airway - blue) are shown.



200

Figure 6: A dose-volume histogram for the AFib treatment plan with 0mm margins added to the target (PTV). The simulated impact of different magnetic field strengths (0 T - solid; 1 T, 3 T - dashed) is shown for the in-line configuration of the linac.

#### 4. Discussion

205

In this letter, we present the first results on target localization in real-time MRI and treatment planning for cardiac radiosurgery with an MRI-Linac. Retrospective analysis of the acquired 2D real-time cine MRI planes shows that it is possible to visualize the target, i.e. the left atrium (LA), during free breathing, localize it in subsequent MRI frames and measure the respiration-induced translation in three dimensions. Our measurements in six healthy volunteers showed a mean respiratory LA motion of 10.2 mm in S-I direction. This aligns with a previous study which found respiration-induced motion of the pulmonary veins (PV) of about 15 mm which generally show higher mobility than the LA itself.<sup>15</sup> Ector *et al.*<sup>15</sup> also found the left and right PV to move differently to each other in the breathing cycle, potentially requiring

210

additional margins for differential motion. But as our intended target is the PV antrum in the relative fixated LA, the differential motion in the target area may be small, requiring further investigation.

MRI offers superior soft tissue contrast, relatively high spatiotemporal resolution and could potentially be used for scar tissue visualization following cardiac ablation.<sup>18</sup> However, it is also prone to imaging artefacts, e.g. caused by flowing blood, and geometric distortions. Flow artefacts can be reduced by optimized cardiac shimming prior to image acquisition. Though image distortions mainly occur in the peripheral region of the FOV, their concrete impact on cardiac tracking accuracy has yet to be determined.<sup>19</sup>

The complexity and challenges of cardiac tracking should not be understated. Cardiac tracking is one of the most challenging problems for image guidance. Not only is the heart beating rapidly causing local deformation, the respiratory system causes motion of the heart of over 1cm per respiratory cycle on average (Table 1). For 2D imaging strategies, both of these motion sources can cause out of plane motion which challenges target identification strategies. The fast motion of the cardiac cycle, and the overlaid respiratory motion, challenges real-time response systems, both in terms of the latency requirements and mechanical constraints. Despite these complexities, on the 8-subject dataset used here, an image-guidance strategy using multiple orthogonal interleaved 2D planes and fast template matching<sup>12</sup> successfully tracked the left atrium. For the real-time response, we have previously demonstrated sub-millimeter accuracy for EPI-based tracking with MLC adaptation for pig irradiation experiments where both respiratory and cardiac motion were included.<sup>20</sup> The latency in the pig tracking study was 400 ms, which matches the estimated upper bound of latency for our current guidance strategy, based on an earlier study on kidney tracking with real-time MRI<sup>12</sup> and 3D-2D template matching reported an acquisition time of 252 ms per 2D plane and a processing/tracking time of another 153 ms (both unoptimized). The results demonstrate that real-time volumetric template matching is feasible.

Though a feasible guidance strategy has been demonstrated, the optimum for MRI-based tracking would be the availability of volumetric anatomical data in real-time. However, the acquisition time in MRI is the main limiting factor for potential real-time applications. For single-plane acquisition, we could reach temporal resolutions down to 50 ms. While ultrasound imaging can create fast 4D information it cannot not provide comparable image quality. Our results are based on the retrospective analysis of single 2D MRI planes, therefore do not render “true” 3D position information. The parallel acquisition of multiple orthogonal planes that we envision for MRI-Linac guidance will yield volumetric data but potentially also increase the acquisition time. An array of image acceleration methods, k-space sampling methods (e.g. radial and spiral), iterative reconstruction of sparse data and the use of priors could all be investigated to improve the spatial and temporal resolution of real-time cardiac MRI guidance for radiotherapy applications. The focus of further MRI studies will be to determine the optimal balance between high spatial resolution and imaging speed and to accelerate current imaging techniques. As local rigidity cannot be assumed in the heart, we see three options to account for cardiac contraction (with ascending complexity):

- (1) An internal target volume (ITV) approach where the magnitude of contractile motion is measured prior to the treatment and accounted for by extending the target structure over all observed cardiac phases. The patient’s breathing would then be compensated by the aforementioned real-time MRI tracking (translation only). This approach potentially increases the dose to surrounding tissues but is the easiest to implement.
- (2) Utilizing the real-time ECG signal for cardiac gating of the treatment delivery as suggested by Wang *et al.*<sup>21</sup> We could utilize the same fast signal processing methods that current scanners are using for cardiac MRI for image acquisition and adapt it to turn the beam on and off according to the diastole gating window, while the respiratory motion would be compensated by MRI tracking. This could spare surrounding tissues better but would also increase treatment time by an estimated 50%. The applicability in arrhythmic patients needs to be determined.
- (3) The tracking process incorporates cardiac deformation, for example through deformable TM. This can be a very time-consuming process, especially in 3D. Another challenge is the sparsity of the volumetric data to drive the deformation since the images acquired during the treatment only show a small number of real-time planes.

For the respiratory-only tracking in (1) and (2), the target motion could be compensated by gating, robotic radiosurgery or dynamic MLC leaf adaption, while the deformation tracking described in (3) requires an MLC.<sup>22</sup> When moving towards tracking and compensation of cardiac motion which may be small in the target area of the LA antrum<sup>23</sup>, prediction will become essential since the cycle length is much shorter than the respiratory cycle. The dosimetric impact of cardiac contraction during treatment delivery must be investigated in order to determine the actual benefit of the different approaches. A study from 2009 suggests that 2 mm margins could compensate for untracked cardiac motion of 1 cm



during robotic radiosurgery.<sup>24</sup> Projecting this to the small LA antrum motion this margin could potentially be reduced to a minimum without the need of tracking or motion compensation, requiring further investigation.

265 The treatment planning for left atrial AFib targets was performed on a single data set, not covering any anatomical variations. While the preliminary findings of this planning study cannot be generalized, they can give first indications about the challenges of cardiac radiosurgery. In our planning study, we have chosen detailed OAR dose limitations of the Grimm *et al.* and the RTOG 0915, which to our knowledge is the most conservative approach.<sup>16</sup> We chose to prescribe 30 Gy to 95% of the PTV in a single fraction according to our previous studies.<sup>7, 25</sup> It is still an open question as to which target dose is really necessary to create a conduction-blocking lesion around the pulmonary veins. The two reported 270 human phase I studies have prescribed a potentially safe 25 Gy for cardiac ablation of ventricular tachycardia<sup>8, 9</sup>, while the most recent animal studies for AF suggested that doses over 30-32.5 Gy might be needed for the treatment to be effective.<sup>5</sup> <sup>7</sup> The transferability of the animal results to human treatment however remains unclear.

Our results indicate that larger margins cause conflicts between the sparing of critical structures and the desired target dose and coverage. The patient selected for this study was an ideal case for cardiac radiosurgery with a medial esophagus 275 location. The esophagus is a very radiosensitive organ lying in direct proximity to the LA. A much smaller distance between target and esophagus and broader margins covering untracked motion might prohibit satisfactory compliance with the planning objectives due to overlapping structures. Planning studies with more data sets will be performed to investigate the inclusion criteria of patient selection for this treatment.

Any clinical radiosurgical cardiac targeting implementation needs to be treated with extreme caution. Radiosurgical 280 treatment of AFib involves high heart doses, and necessarily exceed the RTOG 0915 maximum heart dose for a single fraction (22 Gy). It has been reported that breast cancer patients showed increased cardiac mortality following radiotherapy with differences emerging after 12-15 years post-treatment.<sup>26</sup> While a low toxicity profile was reported for the two cases where patients were successfully treated with cardiac radiosurgery<sup>8, 9</sup>, none of the studies, animal or human, has investigated the long-term effects of the highly localized ablative cardiac dose. Nevertheless, the initial patient cohort 285 might be those with severe comorbidities and too unwell to receive other treatment where the benefit of non-invasive symptom relief might outweigh the potential long-term effects.

## 5. Conclusion

We have presented our initial findings for target localization in real-time MRI and treatment planning for cardiac 290 radiosurgery. Our results indicate that real-time cardiac MRI holds the potential to be used for tracking and that real-time motion compensation is essential to keep margins at a minimum. This is the groundwork towards an entirely non-invasive treatment of atrial fibrillation using an MRI-Linac with real-time image guidance. Our next goal is to build upon the guidance method, integrate with real-time adaption, the initiation of animal studies and eventually human trials to further investigate the potential of this innovative treatment approach.

## 6. Acknowledgements

Supported by NHMRC Australia Fellowship, NHMRC Program Grants and an Endeavour Award. Thanks to Julie Baz and Yuanyuan Ge for improving the manuscript.

## References

- 1 J. Ball, M.J. Carrington, J.J. McMurray, S. Stewart, "Atrial fibrillation: Profile and burden of an evolving epidemic in the 21st century," *International journal of cardiology* **167**, 1807-1824 (2013).
- 2 A.J. Camm, G.Y. Lip, R. De Caterina, I. Savelieva, D. Atar, S.H. Hohnloser, G. Hindricks, P. Kirchhof, J.J. Bax, H. Baumgartner, "2012 focused update of the ESC Guidelines for the management of atrial fibrillation An update of the 2010 ESC Guidelines for the management of atrial fibrillation Developed with the special contribution of the European Heart Rhythm Association," *European heart journal* **33**, 2719-2747 (2012).
- 3 H. Calkins, K.H. Kuck, R. Cappato, J. Brugada, A.J. Camm, S.-A. Chen, H.J. Crijns, R.J. Damiano, D.W. Davies, J. DiMarco, "2012 HRS/EHRA/ECAS Expert Consensus Statement on Catheter and Surgical Ablation of Atrial Fibrillation: Recommendations for Patient Selection, Procedural Techniques, Patient Management and Follow-up, Definitions, Endpoints, and Research Trial Design A report of the Heart Rhythm Society (HRS) Task Force on Catheter and Surgical Ablation of Atrial Fibrillation. ," *Europace*, eus027 (2012).
- 4 A. Sharma, D. Wong, G. Weidlich, T. Fogarty, A. Jack, T. Sumanaweera, P. Maguire, "Noninvasive stereotactic radiosurgery (CyberHeart) for creation of ablation lesions in the atrium," *Heart Rhythm* **7**, 802-810 (2010).
- 5 P.J. Maguire, E. Gardner, A.B. Jack, P. Zei, A. Al-Ahmad, L. Fajardo, E. Ladich, P. Takeda, "Cardiac radiosurgery (CyberHeart™) for treatment of arrhythmia: physiologic and histopathologic correlation in the porcine model," *Cureus* **3**(2011).
- 6 E.A. Gardner, T.S. Sumanaweera, O. Blanck, A.K. Iwamura, J.P. Steel, S. Dieterich, P. Maguire, "In vivo dose measurement using TLDs and MOSFET dosimeters for cardiac radiosurgery," *Journal of Applied Clinical Medical Physics* **13**(2012).
- 7 O. Blanck, F. Bode, M. Gebhard, P. Hunold, S. Brandt, R. Bruder, M. Grossherr, R. Vonthein, D. Rades, J. Dunst, "Dose-Escalation Study for Cardiac Radiosurgery in a Porcine Model," *International Journal of Radiation Oncology\* Biology\* Physics* **89**, 590-598 (2014).
- 8 A. Lo, B. Loo, P. Maguire, S. Soltys, L. Wang, P. Zei, "SBRT for cardiac arrhythmia ablation," *Journal of Radiosurgery & SBRT* **2**(2013).
- 9 J. Cvek, R. Neuwirth, L. Knybel, L. Molenda, B. Otahal, J. Pindor, M. Murárová, M. Kodaj, M. Fiala, M. Branny, "Cardiac Radiosurgery for Malignant Ventricular Tachycardia," *Cureus* **6**(2014).
- 10 A. Schweikard, G. Glosser, M. Bodduluri, M.J. Murphy, J.R. Adler, "Robotic motion compensation for respiratory movement during radiosurgery," *Computer Aided Surgery* **5**, 263-277 (2000).
- 11 R. Yamazaki, S. Nishioka, H. Date, H. Shirato, T. Koike, T. Nishioka, "Investigation of the change in marker geometry during respiration motion: a preliminary study for dynamic-multi-leaf real-time tumor tracking," *Radiation Oncology* **7**, 218 (2012).
- 12 T. Bjerre, S. Crijns, P.M. af Rosenschöld, M. Aznar, L. Specht, R. Larsen, P. Keall, "Three-dimensional MRI-linac intra-fraction guidance using multiple orthogonal cine-MRI planes," *Physics in medicine and biology* **58**, 4943 (2013).
- 13 A. D'Silva, M. Wright, "Advances in imaging for atrial fibrillation ablation," *Radiology research and practice* **2011**(2011).
- 14 D.J. Sher, J.O. Wee, R.S. Punglia, "Cost-Effectiveness Analysis of Stereotactic Body Radiotherapy and Radiofrequency Ablation for Medically Inoperable, Early-Stage Non-Small Cell Lung Cancer," *International Journal of Radiation Oncology\* Biology\* Physics* **81**, e767-e774 (2011).
- 15 J. Ector, S. De Buck, D. Loeckx, W. Coudyzer, F. Maes, S. Dymarkowski, J. Bogaert, H. Heidbüchel, "Changes in Left Atrial Anatomy Due to Respiration: Impact on Three- Dimensional Image Integration During Atrial Fibrillation Ablation," *Journal of cardiovascular electrophysiology* **19**, 828-834 (2008).

- 16 J. Grimm, T. LaCouture, R. Croce, I. Yeo, Y. Zhu, J. Xue, "Dose tolerance limits and dose volume histogram evaluation for stereotactic body radiotherapy," *Journal of Applied Clinical Medical Physics* **12**(2011).
- 17 J. Allison, K. Amako, J. Apostolakis, H. Araujo, P.A. Dubois, M. Asai, G. Barrand, R. Capra, S. Chauvie, R. Chytracek,  
345 "Geant4 developments and applications," *Nuclear Science, IEEE Transactions on* **53**, 270-278 (2006).
- 18 D.C. Peters, J.V. Wylie, T.H. Hauser, K.V. Kissinger, R.M. Botnar, V. Essebag, M.E. Josephson, W.J. Manning,  
"Detection of pulmonary vein and left atrial scar after catheter ablation with three-dimensional navigator-gated delayed  
enhancement mr imaging: initial experience 1," *Radiology* **243**, 690-695 (2007).
- 19 A. Walker, G. Liney, P. Metcalfe, L. Holloway, "MRI distortion: considerations for MRI based radiotherapy treatment  
350 planning," *Australasian Physical & Engineering Sciences in Medicine* **37**, 103-113 (2014).
- 20 P.R. Poulsen, J. Carl, J. Nielsen, M.S. Nielsen, J.B. Thomsen, H.K. Jensen, B. Kjærgaard, P.R. Zepernick, E. Worm, W.  
Fledelius, B. Cho, A. Sawant, D. Ruan, P.J. Keall, "Megavoltage Image-Based Dynamic Multileaf Collimator Tracking  
of a NiTi Stent in Porcine Lungs on a Linear Accelerator," *International Journal of Radiation Oncology • Biology •  
Physics* **82**, e321-e327 (
- 355 21 Z. Wang, C.G. Willett, F.-F. Yin, "Reduction of organ motion by combined cardiac gating and respiratory gating,"  
*International Journal of Radiation Oncology\* Biology\* Physics* **68**, 259-266 (2007).
- 22 Y. Ge, R. O'Brien, C.C. Shieh, J. Booth, P. Keall, "Toward the development of intrafraction tumor deformation tracking  
using a dynamic multi-leaf collimator," *Medical Physics* **41**, 10 (2014).
- 23 A. Brost, W. Wu, M. Koch, A. Wimmer, T. Chen, R. Liao, J. Hornegger, N. Strobel, "Combined cardiac and respiratory  
360 motion compensation for atrial fibrillation ablation procedures," in *Medical Image Computing and Computer-Assisted  
Intervention–MICCAI 2011* (Springer, 2011), pp. 540-547.
- 24 B. Teo, S. Dieterich, O. Blanck, T. Sumanaweera, E. Gardner, "SU- FF- T- 559: Effect of Cardiac Motion On the  
Cyberknife Synchrony Tracking System for Radiosurgical Cardiac Ablation," *Medical Physics* **36**, 2653-2653 (2009).
- 25 R. Werner, F. Bode, R. Bruder, M. Gebhard, J. Dunst, D. Rades, O. Blanck, "Impact of cardiac and respiratory motion  
365 during cardiac radiosurgery: a dose accumulation study in a porcine model," in *ESTRO33 Conference* (Vienna - Austria,  
2014).
- 26 K.H. Tjessem, S. Johansen, E. Malinen, K.V. Reinertsen, T. Danielsen, S.D. Fosså, A. Fosså, "Long-term cardiac  
mortality after hypofractionated radiation therapy in breast cancer," *International Journal of Radiation Oncology\*  
Biology\* Physics* **87**, 337-343 (2013).
- 370

# Catheter ablation

vs.

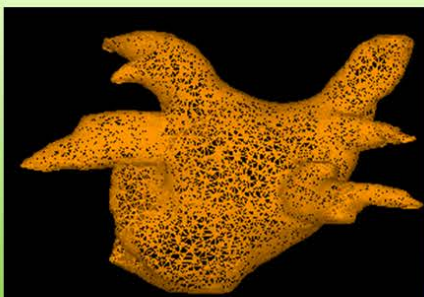
# MRI-Linac treatment

Pre-treatment

CT

MRI (optional)

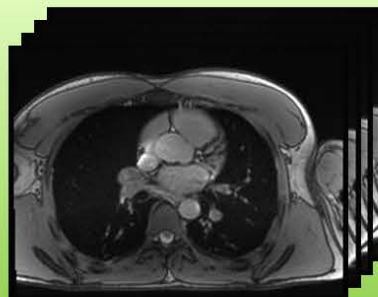
Left atrium model



MRI

CT (optional)

3D left atrium



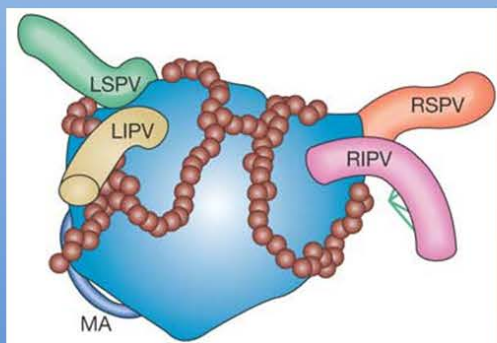
Dose calculations



Treatment session

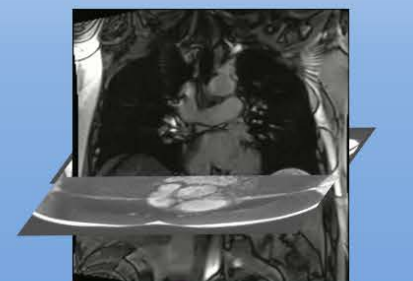
Electrophysiology laboratory

Catheter ablation

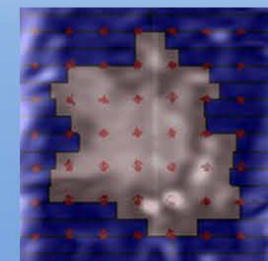


Ablation point locations on "map"

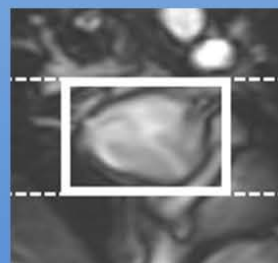
Radiotherapy with MRI tracking:



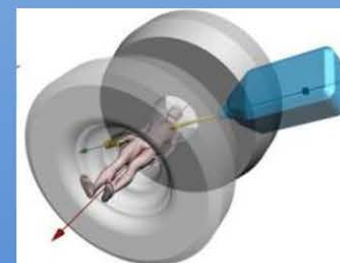
2D real-time MRI



Real-time adaptation



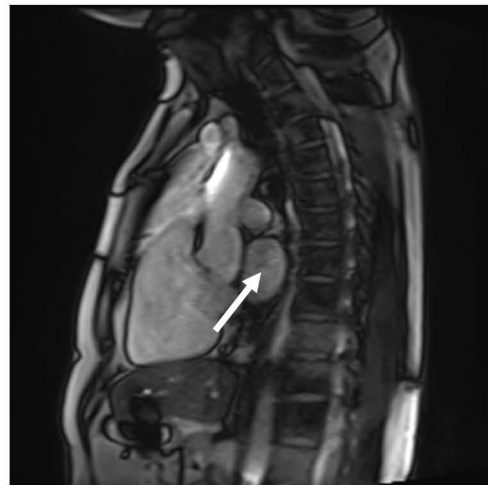
Target position



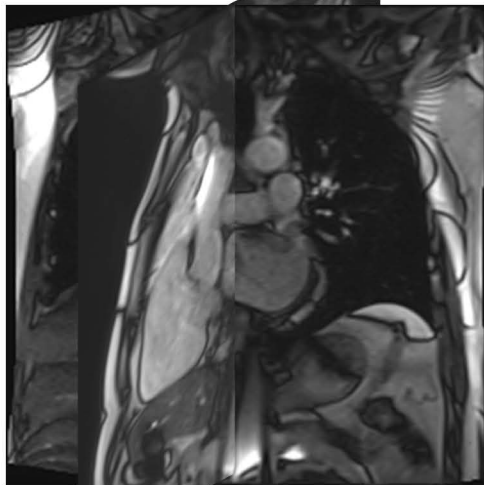
Treatment

Average treatment time  
4-6 hours

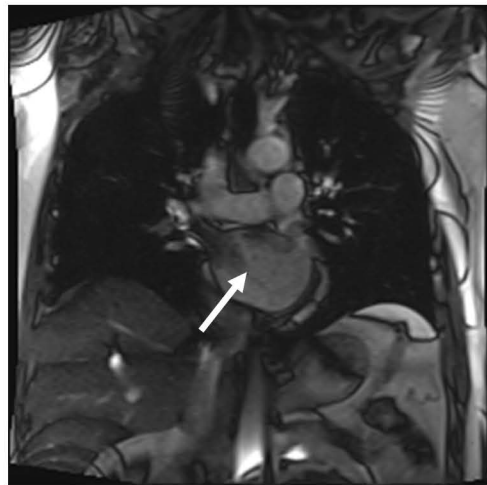
Estimated treatment time <60 minutes



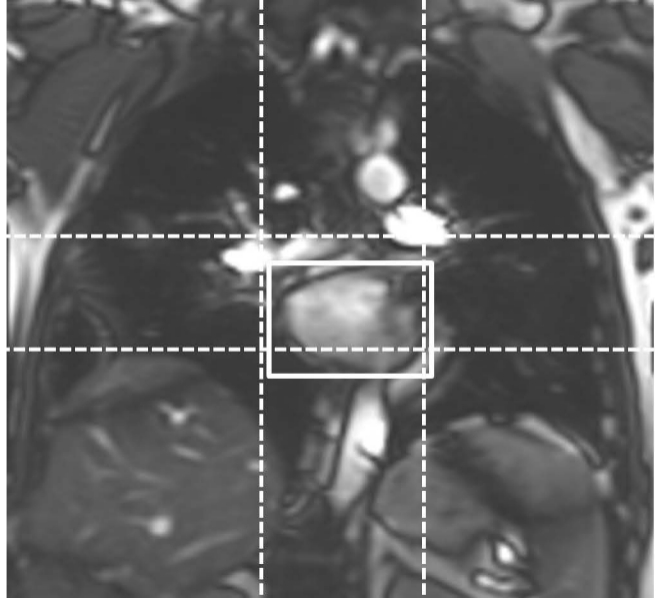
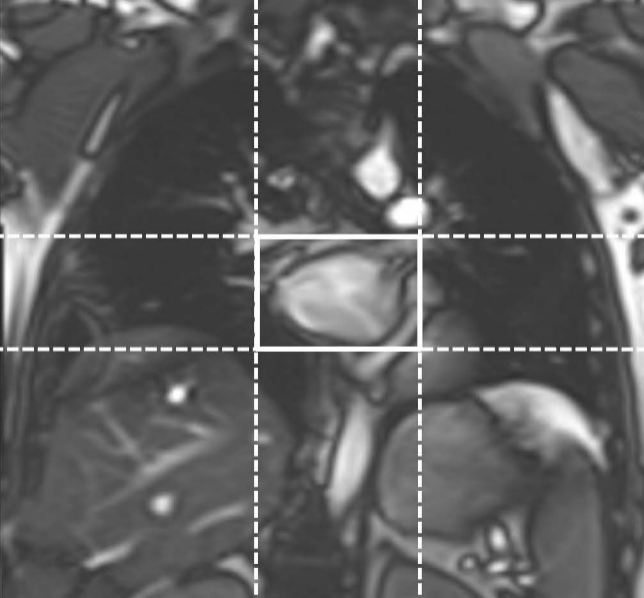
Sagittal

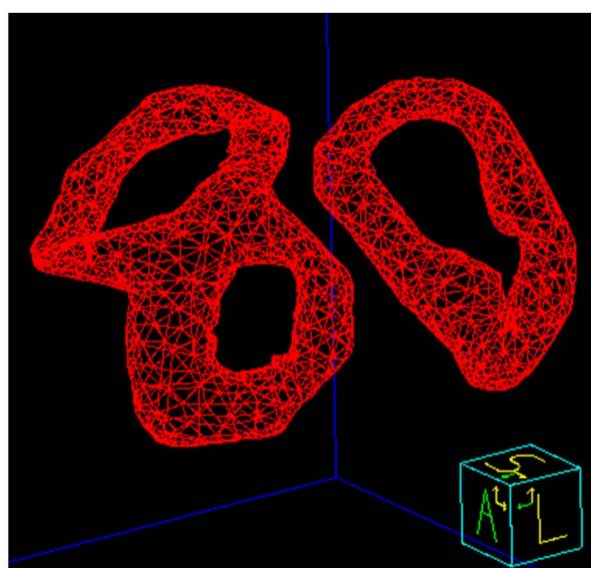


Interleaved



Coronal





**Contours:**

**Target**

**Heart**

**Esophagus**

**Airways**

**Aorta**

**Spinal cord**

